



PERGAMON

International Journal of Solids and Structures 36 (1999) 5013–5027

INTERNATIONAL JOURNAL OF
**SOLIDS and
STRUCTURES**

www.elsevier.com/locate/ijssolstr

Crack kinking in a piezoelectric solid

Ting Zhu*, Wei Yang

Department of Engineering Mechanics, Tsinghua University, Beijing 100084, P.R. China

Received 9 January 1998; in revised form 22 July 1998; accepted 2 August 1998

Abstract

The intrinsic coupling between the mechanical and the electric fields assigns a unique feature for the fracture in a piezoelectric solid. We model the kink of a crack by continuous distribution of edge dislocations and electric dipoles. The problem admits an approach based on the Stroh formalism. A set of coupled singular integral equations are derived for the dislocation and electric dipole density functions associated with a kinked crack. Numerical results indicate that the crack tends to propagate in a straight line under a tensile stress and a positive electric field. For a crack subjected to the mixed mode mechanical loading, a superimposed positive electric field tends to reduce the kink angle. The influence of the non-singular T-stress-charge parallel to a crack is also investigated. It is shown that a transverse tensile stress or a positive transverse electric field will lead to further deviation of the kinked crack from the crack extension line. © 1999 Elsevier Science Ltd. All rights reserved.

1. Introduction

Crack kinking plays an important role in the fracture of piezoelectrics in response to the electro-mechanical loading. Incipient crack kinking in piezoelectric ceramics subjected to an electric field was first reported by McHenry and Koepke (1983). By use of birefringence, Lynch et al. (1995) found that an insulated crack would branch and have a feathered appearance in a sample of 8/65/35 PLZT under a cyclic electric field. Branched crack propagation in multilayer piezoelectric actuators made of $\text{Pb}((\text{Ni}_{1/3}\text{Nb}_{2/3}), \text{Ti}, \text{Zr})\text{O}_3$ was reported by Furuta and Uchino (1993). Park and Sun (1995a) performed three-point bending test with an unsymmetrical crack in a PZT-4 specimen. Their observation indicated that the crack propagation deviated from its original direction under the combined mechanical and electrical loading. Fracture mechanics analyses for a main crack in a piezoelectric solid were presented by many investigators, see Parton (1976), Pak (1990), Sosa (1992), Shindo et al. (1992), Suo et al. (1992), Sosa and Khutoryansky (1996), Zhang et al. (1998), among others. These works cover a wide range of defect orientations, different natures of the applied loads, and various boundary conditions imposed along the crack surface.

* Corresponding author. Fax: 00 86 10 62785569; e-mail: zhut@mail.cic.tsinghua.edu.cn

In mechanics analyses, the method of distributed dislocations is a powerful tool in studying the crack kinking problem. Viewed as a continuous distribution of straight dislocations, the kinked crack in an isotropic linear elastic solid was first attacked by Lo (1978). In the same spirit, Obata et al. (1989) and Azhdari and Nemat-Nasser (1996a, b) analyzed the crack kinking in a linear elastic but anisotropic solid. Extension of this approach to the kinking of an interface crack between dissimilar anisotropic elastic solids was given by Miller and Stock (1989), Wang et al. (1992) and Wang (1994).

The crack kinking in a piezoelectric solid offers a new twist on the method of continuous distribution of dislocations: the distribution of electric potential dislocations (or an electric dipole layer) is required to simulate the electric potential jump across the crack. Barnett and Lothe (1975) generalized the Stroh formalism to include the electric potential jump across the slip plane in piezoelectric materials. Modeling a crack as dislocations and dipoles, Pak (1992) analyzed the electro-elastic field in the vicinity of a crack tip. This approach was recently exploited by Gao et al. (1997) and by Fulton and Gao (1997) to investigate the effect of an electric polarization saturation strip confined in a line segment in front of a crack.

The present paper explores the crack kinking in a piezoelectric solid from a fundamental solution for a dislocation and an electric dipole interacting with a traction-charge free crack. The analysis is confined within the framework of a linear piezoelectric constitutive law. The non-linear effect of the polarization switch is ignored by the assumption of a small scale polarization switching zone. A study addressing the nonlinear switching effect on crack kinking may follow the polarization switching model given by Yang and Zhu (1998) and Zhu and Yang (1997). The plan of the paper is as follows. In Section 2, the solution of a dislocation and an electric dipole interacting with a crack is formulated via the Stroh formalism, whose details are given in Appendix A. The electro-elastic field of a piezoelectric crack is given, and that includes the terms of the T-stress-charge parallel to the crack. A set of coupled singular integral equations are derived for the dislocation and electric dipole density functions associated with a kinked crack. In Section 3, numerical calculations are carried out for the piezoelectric materials under various electro-mechanical loading conditions. The concluding remarks are given in Section 4.

2. Formulation

2.1. Statement of problem

Consider a main crack of length $2a$ contained within an infinite homogeneous piezoelectric medium, as depicted in Fig. 1. The poling direction is normal to the crack faces. The origin of the rectangular coordinate system x_1-x_2 is fixed at the crack center. The x_1 -axis coincides with the crack and the x_2 -axis directs along the poling direction. A kink emanates from the right crack tip and forms an acute angle θ with the x_1 -axis. A kink tip coordinate system, $x'_1-x'_2$, is introduced as shown in Fig. 1. The piezoelectric solid is subjected to remote uniform mechanical and electric loadings. In what follows, a prime denotes differentiation with respect to the corresponding argument, and an overbar represents the complex conjugate. Unless otherwise specified, the indices range from 1 to 3 and summation is implied for the repeated indices.

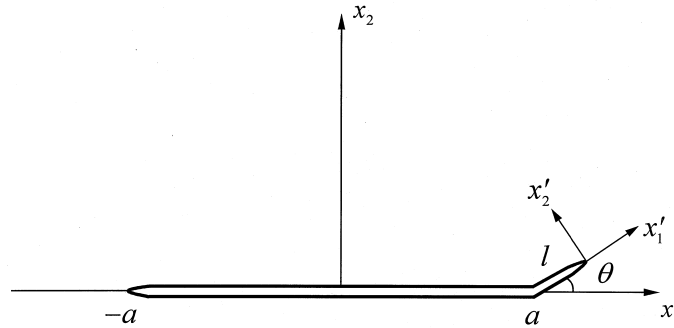


Fig. 1. Schematic illustration of a kinked crack.

2.2. A piezoelectric dislocation interacting with a crack

A kink is modeled by a continuous distribution of dislocations and electric dipoles. A dislocation and an electric dipole located at the same point are termed hereafter the piezoelectric dislocation. The interaction between a piezoelectric dislocation and a traction-charge free crack provides a fundamental solution for the crack kinking in a piezoelectric solid. As shown in Appendix A, all the mechanical and electrical variables in x_1 - x_2 plane can be expressed in terms of three complex potentials $f_i(z)$ ($i = 1, 2, 3$). The one-complex-variable approach (see Suo et al., 1992) is adopted. Namely the arguments of three complex potentials are identical and of the form $z = x_1 + px_2$. Once a solution of $f_i(z)$ is obtained, one may substitute z_i ($z_i = x_1 + p_i x_2, i = 1, 2, 3$) into each complex potential to compute the field quantities. The solution of the complex potential vector \mathbf{f}^{disl} can be built on the superposition of two problems: the solution of a piezoelectric dislocation in an infinite homogeneous piezoelectric solid (labeled by H), and an electro-elastic field to negate the crack surface traction-charge (labeled by N), see Suo (1990)

$$\mathbf{f}^{\text{disl}} = \mathbf{f}^{\text{H}} + \mathbf{f}^{\text{N}} \tag{1}$$

The solution of a piezoelectric dislocation at the point (x_{1d}, x_{2d}) in an infinite homogeneous piezoelectric medium was given by Pak (1992).

$$f_i^{\text{H}}(z) = q_i \ln(z - s_i), \quad s_i = x_{1d} + p_i x_{2d}, \quad i = 1, 2, 3 \tag{2}$$

where

$$\mathbf{q} = [q_1, q_2, q_3] = \frac{1}{2\pi} \mathbf{L}^{-1} (\mathbf{B} + \bar{\mathbf{B}})^{-1} \mathbf{b} \equiv \mathbf{C} \mathbf{b} \tag{3}$$

The expressions for matrices \mathbf{L} and \mathbf{B} are given in (A10) and (A11). The components b_1 and b_2 of the piezoelectric Burgers vector \mathbf{b} are the displacement jumps across the slip plane Δu_1 and Δu_2 , while the component b_3 represents the electric potential jump $\Delta \phi$.

From eqn (A14) in Appendix A, the traction-charge along the x_1 -axis is

$$\mathbf{t}^{(2)}(x_1) = \{\sigma_{21}, \sigma_{22}, D_2\} = 2 \text{Re} [\mathbf{L} \mathbf{f}'^{\text{H}}(x_1)] \tag{4}$$

To negate this traction-charge along the crack faces, a solution based on the complex potentials \mathbf{f}^{N} should be superimposed. The exact negation provides the following equation for \mathbf{f}^{N}

$$\mathbf{L}\mathbf{f}^{\text{N}'}(z) = -\frac{\chi(z)}{2\pi i} \int_{-a}^a \frac{\mathbf{t}^{(2)}(x_1)}{\chi^+(x_1)(x_1-z)} dx_1 + \mathbf{P}\chi(z) \quad (5)$$

where

$$\chi(z) = \frac{1}{\sqrt{z^2 - a^2}} \quad (6)$$

and the constant vector \mathbf{P} is yet to be determined. Substituting eqn (4) into eqn (5), one can evaluate the above integral and arrive at

$$f_i^{\text{N}'}(z) = \frac{1}{2}(U_{ij} + V_{ij})b_j \quad (7)$$

where

$$U_{ij} = C_{ij} \left[\frac{1}{z-s_i} \left(\frac{\chi(z)}{\chi(s_i)} - 1 \right) \right], \quad \text{no sum on } i \quad (8)$$

$$V_{ij} = \sum_{n=1}^3 L_{im}^{-1} \overline{L_{mn}} C_{nj} \left[\frac{1}{z-\bar{s}_n} \left(\frac{\chi(z)}{\chi(\bar{s}_n)} - 1 \right) \right] \quad (9)$$

The constant vector \mathbf{P} is determined from the requirement that the displacement be single-valued (for a circuit taken around the crack and the piezoelectric dislocation, see Lo, 1978; Zhang and Li, 1991), and given by

$$\mathbf{P} = -\frac{1}{4\pi} [(\mathbf{B} + \bar{\mathbf{B}})^{-1} + \overline{(\mathbf{B} + \bar{\mathbf{B}})^{-1}}] \mathbf{b} \quad (10)$$

2.3. Electro-elastic field of a piezoelectric crack

The electro-elastic field of a piezoelectric crack was presented by Sosa (1992) and by Park and Sun (1995b). The solution given in this subsection will emphasize the non-singular T-stress-charge parallel to the crack. Consider a crack of length $2a$ in an infinite piezoelectric medium subjected to remote uniform electro-mechanical loadings

$$\mathbf{t}^{(1)\infty} = \{\sigma_{11}^{\infty}, \sigma_{12}^{\infty}, D_1^{\infty}\} \quad (11)$$

and

$$\mathbf{t}^{(2)\infty} = \{\sigma_{21}^{\infty}, \sigma_{22}^{\infty}, D_2^{\infty}\} \quad (12)$$

The problem can be solved by superposition. One first solves the problem without the crack and determines the stress-charge on the prospective crack line. The negating stress-charge is subsequently applied to the crack faces. The corresponding potentials for the latter problem are given by

$$\mathbf{f}^{\text{crack}'}(z) = \frac{1}{2} \mathbf{L}^{-1} \mathbf{t}^{(2)\infty} \left(\frac{z}{\sqrt{z^2 - a^2}} - 1 \right) \quad (13)$$

The solution has to be converted from the one-complex-variable form into three-complex-variable representation. The stress and electric induction vectors are given by, also see eqns (A6) and (A7)

$$t_i^{(2)\text{crack}} = \text{Re} \sum_{k=1}^3 L_{ik} L_{kj}^{-1} t_j^{(2)\infty} \frac{z_k}{\sqrt{z_k^2 - a^2}} \quad (14)$$

and

$$T_i^{(1)\text{crack}} = T_i - \text{Re} \sum_{k=1}^3 L_{ik} L_{kj}^{-1} t_j^{(2)\infty} p_k \frac{z_k}{\sqrt{z_k^2 - a^2}} \quad (15)$$

In eqn (15), T_i represents the non-singular T-stress-charge vector in the expansion of the crack tip electro-elastic field. It is given by

$$T_i = t_i^{(1)\infty} + \text{Re} \sum_{k=1}^3 L_{ik} L_{kj}^{-1} t_j^{(2)\infty} p_k \quad (16)$$

In deriving the above results, the crack is assumed to be traction free and electric impermeable, namely:

$$\sigma_{12} = \sigma_{22} = D_2 = 0, \quad x_1 \in (-a, a) \quad (17)$$

The validity of the electric impermeable assumption was discussed by Pak (1990) and by Suo et al. (1992). An impermeable crack requires no external charge on either crack face and negligible electric induction inside the flaw. The electro-elastic analyses that incorporate the electric field within the flaw have been pursued by many investigators, for example see Sosa and Khutoryansky (1996), Zhu and Yang (1997), and Zhang et al. (1998). The results suggest that the impermeable formulation can be derived as a particular case of the exact model. As the first attempt to investigate the crack kinking in a piezoelectric solid, we will regard both the main crack and the kink impermeable.

The traction free condition will no longer hold when the upper and lower faces of the crack come into contact. Define the displacement and electric potential jumps across the crack as

$$\mathbf{d}(x_1) = \mathbf{u}^+(x_1) - \mathbf{u}^-(x_1) \quad (18)$$

From eqns (A11) and (13), one may derive the jumps in displacements and electric potential. The leading terms of them are given by:

$$\mathbf{d}(r) = \sqrt{2ar} \mathbf{H} \mathbf{t}^{(2)\infty} \quad (19)$$

where r represents a distance behind the crack tip. The 3×3 matrix \mathbf{H} is given by

$$\mathbf{H} = \mathbf{B} + \bar{\mathbf{B}} \quad (20)$$

Since $H_{21} = 0$ (see Suo et al., 1992), the condition for an open crack requires that

$$\frac{D_2^\infty}{\sigma_{22}^\infty} > -\frac{H_{22}}{H_{23}} \quad (21)$$

For the crack closure induced by a negative electric field, the kinking problem may be solved by modeling the main crack together with the kink as a continuous distribution of dislocations, parallel to the analysis given by Hayashi and Nemat-Nasser (1981) for the crack kinking from an interface crack.

2.4. Singular integral equations

A kink of length l is modeled by continuous distribution of piezoelectric dislocations. Based on the solution of a piezoelectric dislocation interacting with a crack and the solution of a piezoelectric crack, the problem of a kinked crack can be solved through singular integral equations. The traction free and electric impermeable surface condition of the main crack is satisfied by the solutions in the previous subsections. Along the kink, we require that

$$\sigma_{1'2'} = \sigma_{2'2'} = D_{2'} = 0, \quad x' \in (0, l) \quad (22)$$

A set of coupled singular integral equations can be derived by enforcing these conditions

$$\int_0^l \frac{M_{ij} b_j}{x' - \zeta} d\zeta + \int_0^l K_{ij} b_j d\zeta = -t_i^{(2)\text{crack}} \quad (23)$$

where

$$M_{1j} = 2 \operatorname{Re} \sum_{k=1}^3 \left[\frac{\Omega_k}{\omega_k} C_{kj} \right], \quad M_{2j} = 2 \operatorname{Re} [\omega_k C_{kj}], \quad M_{3j} = 2 \operatorname{Re} [\lambda_k C_{kj}] \quad (24)$$

$$K_{1j} = \operatorname{Re} [\Omega_k (U_{kj} + V_{kj})], \quad K_{2j} = \operatorname{Re} [\omega_k^2 (U_{kj} + V_{kj})], \quad K_{3j} = \operatorname{Re} \sum_{k=1}^3 [\lambda_k \omega_k (U_{kj} + V_{kj})] \quad (25)$$

$$\omega_k = \cos \theta + p_k \sin \theta \quad (26)$$

$$\Omega_k = (1 - p_k^2) \sin \theta \cos \theta - p_k \cos 2\theta \quad (27)$$

In the right hand side of eqn (23), the $t_i^{(2)\text{crack}}$ term represents the stress and electric induction due to the presence of the main crack, and is expressed by the local coordinates x' . In eqn (23), the dislocation densities $b_1(\zeta)$, $b_2(\zeta)$ and the electric dipole density $b_3(\zeta)$ are unknown. We extract the singularity from $b_k(\zeta)$ by

$$b_k(\zeta) = \frac{\hat{b}_k(\zeta)}{\sqrt{\zeta(l-\zeta)}} \quad (28)$$

where $\hat{b}_k(\zeta)$ are the non-singular parts of $b_k(\zeta)$. The singularity at the kink root is considered to be less than one half, based on the singularity analysis of Bogy (1971). Hence, the end value $\hat{b}_k(0)$ can be taken as zero. The numerical method of Erdogan (1978) is used to solve the singular equations. Once the density functions of piezoelectric dislocations are known, the intensity factors for stress and electric induction at the kink tip can be obtained by

$$\mathbf{k} = (K_{II}, K_I, K_D) = \pi \sqrt{\frac{2\pi}{l}} \mathbf{M}\hat{\mathbf{b}}(l) \quad (29)$$

where

$$\hat{\mathbf{b}}(l) = \{\hat{b}_1(l), \hat{b}_2(l), \hat{b}_3(l)\} \quad (30)$$

are the values of $\hat{b}_i(\zeta)$ at the kink tip and the matrix M_{ij} is defined in eqn (24).

3. Results and discussion

The material constants of PZT-4, as listed in Appendix B, are used in the calculations. A far field electric displacement boundary condition is adopted. The present formulation is suitable to investigate the effect of a *positive* electric field ($D_2^\infty > 0$) on the kinking behavior of piezoelectrics. A negative electric field may lead to crack surface contact, then invalidate the electro-elastic field given in the last section. For PZT-4, the condition (21) requires that $D_2^\infty/\sigma_{22}^\infty > -0.789 \times 10^{-9}$ C/N. A negative electric field within this range has little effect on the crack kinking of PZT-4. Moreover, the scale of the polarization switching zone under a negative electric field is much larger than that under a positive electric field of the same intensity (see Yang and Zhu, 1998; Zhu and Yang, 1997). Therefore, the non-linear effect of polarization switching should not be ignored for the cracking of piezoelectrics under a negative electric field.

Different criteria have been proposed to predict the direction of crack kinking. Commonly used fracture criteria, such as kinking along the direction of the maximum K_I , the zero K_{II} , the maximum hoop stress and the maximum energy release rate, lead to similar prediction of crack propagation path for a crack in an isotropic material. However, these criteria may predict different kinking angles for anisotropic materials. Azhdari and Nemat-Nasser (1996b) made a thorough study on various criteria. They found that a K -based fracture criterion, in some cases, does not yield the same result as the one obtained by an energy based criterion. For piezoelectrics, it is shown that the K -based criterion and the energy based criterion differ when the energetics of the electric field is taken into account, see Pak (1992) and Zhang et al. (1998). Furthermore, considering the electric ductility of piezoelectrics, Gao et al. (1997) and Fulton and Gao (1997) verified that the global energy release rate differs from the energy release rate calculated from the crack tip. In the present paper, the maximum mode I kink tip stress intensity factor (SIF) criterion is adopted to predict the kinking direction.

We first consider a piezoelectric crack with an infinitesimal kink length, $a/l = 10^6$. Figures 2 and 3 plot the mode I and II SIFs at the kink tip, normalized by $K_0 = \sigma_{22}^\infty \sqrt{\pi a}$, under different positive electric fields. The maximum of the mode I SIF always occurs at $\theta = 0$. If the fracture toughness of a piezoelectric solid is isotropic, the crack will propagate in a straight line under a tensile stress and a positive electric field. Due to electro-mechanical coupling, a pure mechanical loading can also induce an electric displacement intensity factor at the kink tip, as shown in Fig. 4.

Next, we consider a kinked crack which is induced by an initial defect or an asymmetric load. Figure 5 plots the mode I kink tip SIFs for different kink lengths. The angles of the kinks are chosen to be $0, \pi/6$ and $\pi/4$. As expected, the electric field has no influence on the SIF when $\theta = 0$.

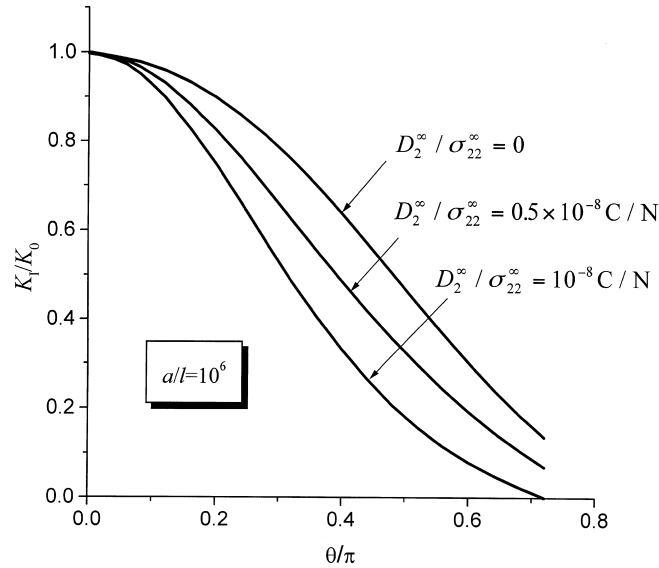


Fig. 2. Mode I SIF at the kink tip for a kinked crack under a tensile and a positive electric field, $K_0 = \sigma_{22}^\infty \sqrt{\pi a}$.

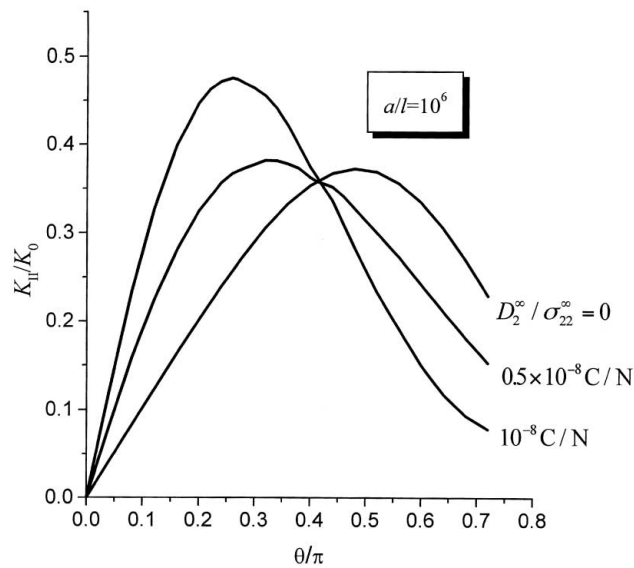


Fig. 3. Mode II SIF at the kink tip for a kinked crack under a tensile stress and a positive electric field.

For $\theta = \pi/6$ and $\pi/4$, the effect of a positive electric field, i.e., $D_2^\infty / \sigma_{22}^\infty = 10^{-8} \text{ C/N}$, is to lower the kink tip SIF when the kink length is small. Azhdari and Nemat-Nasser (1996b) verified that SIFs at the tip of a vanishingly small kink would become independent of the small length l . Figure 5 confirms that K_I approaches an asymptote as $a/l \rightarrow \infty$, and extends the same conclusion to a

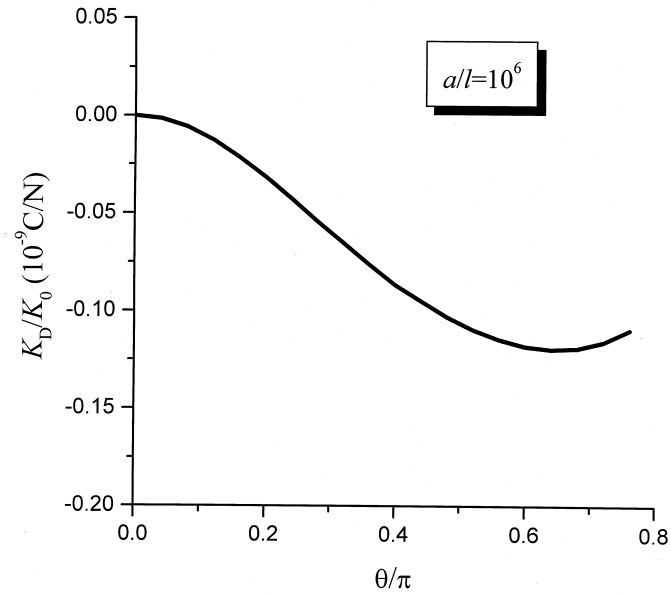


Fig. 4. Electric displacement intensity factor at the kink tip induced by a tensile stress field.

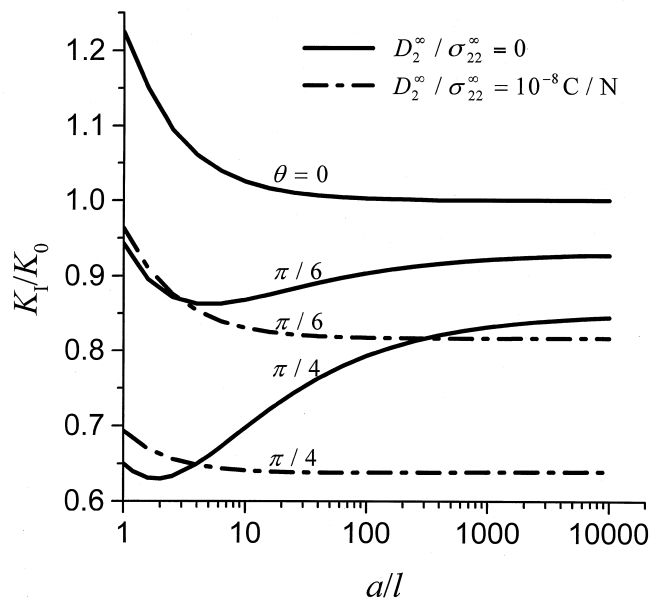


Fig. 5. Mode I kink tip SIF vs the kink length.

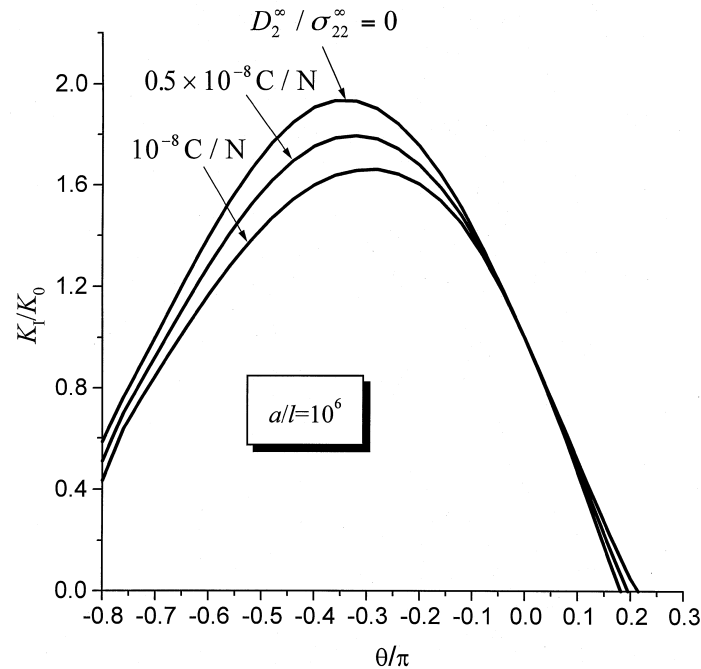


Fig. 6. Mode I kink tip SIF for a kinked crack under a mixed mode mechanical loading ($\sigma_{12}^\infty = \sigma_{22}^\infty$) and a positive electric field.

piezoelectric medium. As the kink length increases, the SIF at the kink tip rises monotonically under a sufficiently large positive electric field. With a further increase of the kink length, the applied positive electric field might cause a SIF at the kink tip that exceeds the one under a pure mechanical loading.

Crack kinking will occur in piezoelectrics under an asymmetric mechanical loading. Park and Sun (1995a) observed crack kinking in a three-point bending test with an asymmetric crack in a PZT-4 specimen. In the following calculation, the far field shear stress is chosen to be equal to the tensile stress. Figure 6 depicts the variation of the mode I kink tip SIF for an infinitesimal small kink length $a/l = 10^6$. The maximum value of SIF is achieved at an angle of -65° . Thus, the crack will propagate in an oblique path. Furthermore, one can observe the effect of positive electric fields on kinking from Fig. 6. Both the kink tip SIF and the kink angle will decrease with the rise of applied positive electric fields.

The stress parallel to a crack may bear considerable effect on crack kinking in elastic materials, as addressed by Cotterell and Rice (1980), Gao and Chiu (1992) and Wang (1994). For piezoelectrics under a mixed mode mechanical loading ($\sigma_{12}^\infty = \sigma_{22}^\infty$), the effects of the transverse stresses on the variation of kink tip SIFs are shown in Fig. 7, and the effects of the transverse electric fields on the kink tip SIFs are given in Fig. 8. It can be seen that a transverse tensile stress or a positive transverse electric field will enlarge the kink angle, while a transverse compress stress or a negative transverse electric field will reduce the kink angle.

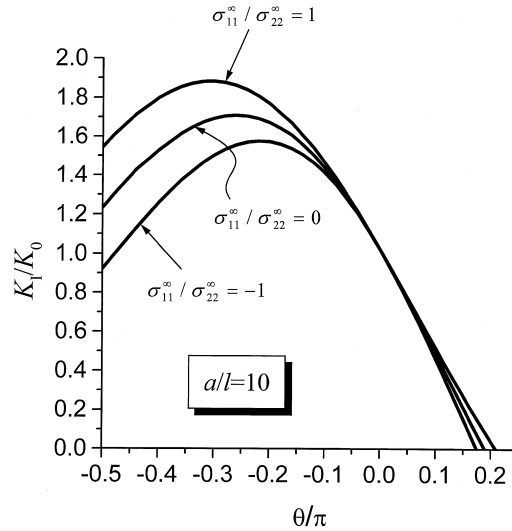


Fig. 7. Effect of a transverse stress on the variation of the mode I kink tip SIF for a kinked crack under a mixed mode mechanical loading ($\sigma_{12}^\infty = \sigma_{22}^\infty$).

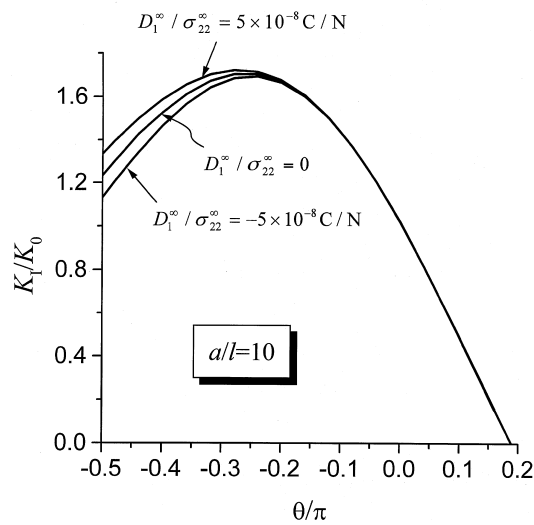


Fig. 8. Effect of a transverse electric field on the variation of the mode I kink tip SIF for a kinked crack under a mixed mode mechanical loading ($\sigma_{12}^\infty = \sigma_{22}^\infty$).

4. Conclusion

The present investigation models the kink of a crack by continuous distribution of edge dislocations and electric dipoles. The problem admits an approach based on the Stroh formalism. A set of coupled singular integral equations are derived for the dislocation and electric dipole density

functions associated with a kinked crack. Numerical results indicate that the crack tends to propagate in a straight line under a tensile stress and a positive electric field. For a crack subjected to a mixed mode mechanical loading, a superimposed positive electric field normal to the crack tends to reduce the kink angle. The non-singular T-stress-charge parallel to a crack also affects its kinking behavior. A transverse tensile stress or a positive transverse electric field will enlarge the kinking angle from the crack extension line, while a transverse compressive stress or a negative transverse electric field will reduce it.

Acknowledgement

This work was supported by the National Natural Science Foundation of China.

Appendix A: Stroh formalism for in-plane piezoelectric problem

Barnett and Lothe (1975) and Suo et al. (1992) have formulated the general solution of a linear piezoelectric material. Introduce a material coordinate system (X_1, X_2, X_3) , where the poling direction is parallel to the X_3 -axis. Attention is focused on the field in X_1 – X_3 plane, where the out-of-plane displacement does not couple with the in-plane displacements and the electric potential. For convenience, the X_1 – X_3 plane is re-labelled as x_1 – x_2 plane in analysis. A general solution in x_1 – x_2 plane is given by

$$\mathbf{u} = \{u_1, u_2, \phi\} = \mathbf{a}f(z) \quad (\text{A1})$$

where

$$z = x_1 + px_2 \quad (\text{A2})$$

The number p and the column \mathbf{a} are determined by

$$[\mathbf{Q} + (\mathbf{R} + \mathbf{R}^T)p + \mathbf{T}p^2]\mathbf{a} = 0 \quad (\text{A3})$$

where the 3×3 matrices \mathbf{Q} , \mathbf{R} and \mathbf{T} are

$$\mathbf{Q} = \begin{bmatrix} c_{11} & 0 & 0 \\ 0 & c_{44} & e_{15} \\ 0 & e_{15} & -\kappa_{11} \end{bmatrix}, \quad \mathbf{R} = \begin{bmatrix} 0 & c_{13} & e_{31} \\ c_{44} & 0 & 0 \\ e_{15} & 0 & 0 \end{bmatrix}, \quad \mathbf{T} = \begin{bmatrix} c_{44} & 0 & 0 \\ 0 & c_{33} & e_{33} \\ 0 & e_{33} & -\kappa_{33} \end{bmatrix} \quad (\text{A4})$$

Note that the elastic, piezoelectric and dielectric constants in the above matrices are represented in the material coordinate system (X_1, X_2, X_3) . Equation (A3) corresponds to an eigenvalue problem. Let p_1, p_2 and p_3 be the roots with positive imaginary parts of the eigen-equation, \mathbf{a}_i the associated columns, and $z_i = x_1 + p_i x_2$. The displacement and electric potential are expressed by

$$\mathbf{u} = 2 \operatorname{Re} \sum_{i=1}^3 \mathbf{a}_i f_i(z_i) \quad (\text{A5})$$

The stress and induction are given by

$$\mathbf{t}^{(1)} = \{\sigma_{11}, \sigma_{12}, D_1\} = -2 \operatorname{Re} \sum_{i=1}^3 \mathbf{l}_i p_i f'_i(z_i) \quad (\text{A6})$$

$$\mathbf{t}^{(2)} = \{\sigma_{21}, \sigma_{22}, D_2\} = 2 \operatorname{Re} \sum_{i=1}^3 \mathbf{l}_i f'_i(z_i) \quad (\text{A7})$$

where the columns \mathbf{l}_i are given by

$$\mathbf{l}_i = (\mathbf{R}^T + p_i \mathbf{T}) \mathbf{a}_i = \frac{-1}{p_i} (\mathbf{Q} + p_i \mathbf{R}) \mathbf{a}_i \quad (\text{A8})$$

Define 3×3 matrices

$$\mathbf{A} = [\mathbf{a}_1, \mathbf{a}_2, \mathbf{a}_3], \quad \mathbf{L} = [\mathbf{l}_1, \mathbf{l}_2, \mathbf{l}_3] \quad (\text{A9})$$

Every column \mathbf{a}_i is uniquely determined up to a complex-valued multiplicative constant, that allows the following normalization:

$$\mathbf{L} = \begin{bmatrix} -p_1 & -p_2 & -p_3 \\ 1 & 1 & 1 \\ \lambda_1 & \lambda_2 & \lambda_3 \end{bmatrix} \quad (\text{A10})$$

Define a 3×3 matrix \mathbf{B}

$$\mathbf{B} = i\mathbf{A}\mathbf{L}^{-1} \quad (\text{A11})$$

Following the one-complex-variable approach by Suo et al. (1992), we introduce a column of a single variable defined as

$$\mathbf{f}(z) = [f_1(z), f_2(z), f_3(z)] \quad (\text{A12})$$

It follows that

$$\mathbf{u} = 2 \operatorname{Re} [\mathbf{A}\mathbf{f}] \quad (\text{A13})$$

$$\mathbf{t}^{(2)} = 2 \operatorname{Re} [\mathbf{L}\mathbf{f}'] \quad (\text{A14})$$

Appendix B

Material constants for PZT-4 piezoelectric ceramics (Park and Sun, 1995a) are used in numerical calculations.

Elastic constants:

$$c_{11} = 13.9 \times 10^{10} \text{ N/m}^2, \quad c_{33} = 11.3 \times 10^{10} \text{ N/m}^2, \quad c_{12} = 7.78 \times 10^{10} \text{ N/m}^2$$

$$c_{13} = 7.43 \times 10^{10} \text{ N/m}^2, \quad c_{44} = 2.56 \times 10^{10} \text{ N/m}^2$$

$$c_{66} = \frac{1}{2}(c_{11} - c_{12}) = 3.06 \times 10^{10} \text{ N/m}^2$$

Piezoelectric constants:

$$e_{33} = 13.84 \text{ C/m}^2, \quad e_{31} = -6.98 \text{ C/m}^2, \quad e_{15} = 13.44 \text{ C/m}^2$$

Dielectric constants:

$$\kappa_{11} = 6.00 \times 10^{-9} \text{ F/m}, \quad \kappa_{33} = 5.47 \times 10^{-9} \text{ F/m}$$

References

- Azhdari, A., Nemat-Nasser, S., 1996a. Hoop stress intensity factor and crack kinking in anisotropic brittle solids. *Int. J. Solids Struct.* 33, 2023–2037.
- Azhdari, A., Nemat-Nasser, S., 1996b. Energy-release rate and crack kinking in anisotropic brittle solids. *J. Mech. Phys. Solids* 44, 929–951.
- Barnett, D.M., Lothe, J., 1975. Dislocations and line charges in anisotropic piezoelectric insulators. *Phys. Status Solidi (b)* 67, 105–111.
- Bogy, D.B., 1971. Two edge-bonded elastic wedges of different materials and wedge angles under surface tractions. *J. Appl. Mech.* 38, 377–386.
- Cotterell, B., Rice, J.R., 1980. Slightly curved or kinked cracks. *Int. J. Fract.* 11, 708–712.
- Erdogan, F., 1978. Mixed boundary-value problem in mechanics. In: Nemat-Nasser, S. (Ed.), *Mechanics Today*. Pergamon Press, 4, 1–86.
- Fulton, C.C., Gao, H., 1997. Electrical nonlinearity in fracture of piezoelectric ceramics. *Appl. Mech. Rev.* 50, S56–S63.
- Furuta, A., Uchino, K., 1993. Dynamic observation of crack propagation in piezoelectric multilayer actuators. *J. Am. Ceram. Soc.* 76, 1615–1617.
- Gao, H., Chiu, C., 1992. Slightly curved or kinked cracks in anisotropic elastic solids. *Int. J. Solids Struct.* 29, 947–972.
- Gao, H., Zhang, T.Y., Tong, P., 1997. Local and global energy rates for an electrically yielded crack in piezoelectric ceramics. *J. Mech. Phys. Solids* 45, 491–510.
- Hayashi, K., Nemat-Nasser, S., 1981. On branched, interface cracks. *J. Appl. Mech.* 48, 529–533.
- Lo, K.K., 1978. Analysis of branched cracks. *J. Appl. Mech.* 45, 797–802.
- Lynch, C.S., Yang, W., Collier, L., Suo, Z., McMeeking, R.M., 1995. Electric field induced cracking in ferroelectric ceramics. *Ferroelectrics* 166, 11–30.
- McHenry, K.D., Koepke, B.G., 1983. Electric field effects on subcritical crack growth in PZT. *Frac. Mech. Ceram.* 5, 337–352.
- Miller, G.R., Stock, W.L., 1989. Analysis of branched interface cracks between two dissimilar anisotropic media. *J. Appl. Mech.* 56, 844–849.
- Obata, M., Nemat-Nasser, S., Goto, Y., 1989. Branched cracks in anisotropic elastic solids. *J. Appl. Mech.* 56, 858–864.
- Pak, Y.E., 1990. Crack extension force in a piezoelectric material. *J. Appl. Mech.* 57, 647–653.
- Pak, Y.E., 1992. Linear electro-elastic fracture mechanics of piezoelectric materials. *Int. J. Fract.* 54, 79–100.
- Park, S.B., Sun, C.T., 1995a. Fracture criteria for piezoelectric ceramics. *J. Am. Ceram. Soc.* 78, 1475–1480.
- Park, S.B., Sun, C.T., 1995b. Effect of electric field on fracture of piezoelectric ceramics. *Int. J. Fract.* 70, 203–216.
- Parton, V.Z., 1976. Fracture mechanics of piezoelectric materials. *Acta Astronaut.* 3, 671–683.
- Shindo, Y., Ozawa, E., Nowacki, J.P., 1990. Similar stress and electric fields of a cracked piezoelectric strip. *Appl. Electromagn. Mater.* 1, 77–87.
- Sosa, H., 1992. On the fracture mechanics of piezoelectric solids. *Int. J. Solids Struct.* 29, 2613–2622.
- Sosa, H., Khutoryansky, N., 1996. New developments concerning piezoelectric materials with defects. *Int. J. Solids Struct.* 33, 3399–3414.
- Suo, Z., 1990. Singularities, interfaces and cracks in dissimilar anisotropic media. *Proc. R. Soc. Lond.* A427, 331–358.
- Suo, Z., Kuo, C.-M., Barnett, D.M., Willis, J.R., 1992. Fracture mechanics for piezoelectric ceramics. *J. Mech. Phys. Solids* 40, 739–765.

- Wang, T.C., 1994. Kinking of an interface crack between two dissimilar anisotropic elastic solids. *Int. J. Solids Struct.* 31, 629–641.
- Wang, T.C., Shih, C.F., Suo, Z., 1992. Crack extension and kinking in laminates and bicrystals. *Int. J. Solids Struct.* 29, 327–344.
- Yang, W., Zhu, T., 1998. Switch-toughening of ferroelectrics under electric field. *J. Mech. Phys. Solids* 46, 291–311.
- Zhang, T.Y., Li, J.C.M., 1991. Image forces and shielding effects of an edge dislocation near a finite length crack. *Acta Metall. Mater.* 39, 2379–2744.
- Zhang, T.Y., Qian, C.F., Tong, P., 1998. Linear electro-elastic analysis of a cavity of a crack in a piezoelectric material. *Int. J. Solids Struct.* 35, 2121–2149.
- Zhu, T., Yang, W., 1997. Toughness variation of ferroelectrics by polarization switch under non-uniform electric field. *Acta Mater.* 45, 4695–4702.